in the d-wave channel for the $t-J$-model taking into account the preexponential factor — opens up an interesting possibility for studying the T_c-vs-x curve for HTSC systems as a BCS – BEC crossover for the pairing of two composite holes in the d-wave channel.

7. Conclusion

Concluding we briefly outline the main results presented in this report. Based on the resonance ($a \gg r_0$) approximation, we derived and exactly solved integral equations for trios and quartets in the 3D and 2D cases. We calculated the scattering amplitude of a molecule from a molecule in a 3D and 2D resonant Fermi gas, and we determined bound state energies for all the possible three- or four-particle complexes in the 2D case. As a result, we were able to construct the phase diagrams for a resonant Fermi gas and a resonant Fermi – Bose mixture. We also proposed a new superconductivity scenario for HTSC systems, in which two composite holes, each containing a spinon and a holon, form a superconducting pair in the d-wave channel.

Acknowledgments. The authors acknowledge fruitful discussions with A F Andreev, Yu Kagan, L V Keldysh, F Nosieres, P Woelfle, D Vollhardt, I A Fomin, G V Shlyapnikov, P Fulde, L P Pitaevskii, and C Salomon. The work was supported by the Russian Foundation for Basic Research (grant No. 06-02-16449).

References

1. Pitaevskii L, Stringari S *Bose–Einstein Condensation* (Oxford: Clarendon Press, 2003); Dalfovo F, Giorgini S, Pitaevskii L P, Stringari S *Rev. Mod. Phys.* **71** 463 (1999)
2. Inouye S et al. *Nature* **392** 151 (1998)
3. Kagan M Yu et al. *Phys. Rev. A* **70** 023607 (2004)
4. Kagan M Yu, Efremov D V *Phys. Rev. B* **65** 195103 (2002)
5. Greiner M, Regal C A, Jin D S *Nature* **426** 537 (2003); Inouye S et al. *Phys. Rev. Lett.* **93** 183201 (2004)
6. Zwierlein M W et al. *Phys. Rev. Lett.* **91** 250401 (2003)
7. Jochim S et al. *Science* **302** 2101 (2003)
8. Bourdel T et al. *Phys. Rev. Lett.* **93** 050401 (2004)
9. Bulaevskii L N, Nagaev E L, Khomskii D I *Zh. Eksp. Teor. Fiz.* **54** 1562 (1968) [*Sov. Phys. JETP* **27** 836 (1968)]
10. Brinkman W F, Rice T M *Phys. Rev. B* **2** 1324 (1970)
11. Skorniakov G V, Ter-Martirosian K A *Zh. Eksp. Teor. Fiz.* **31** 775 (1956) [*Sov. Phys. JETP* **4** 648 (1957)]
12. Brodsky I V et al. *Pis'ma Zh. Eksp. Teor. Fiz.* **82** 306 (2005) [*JETP Lett.* **82** 273 (2005)]; *Phys. Rev. A* **73** 032724 (2006)
13. Danilov G S *Zh. Eksp. Teor. Fiz.* **40** 498 (1961) [*Sov. Phys. JETP* **13** 349 (1961)]
14. Minlos R A, Faddeev L D *Zh. Eksp. Teor. Fiz.* **41** 1850 (1961) [*Sov. Phys. JETP* **14** 1315 (1962)]
15. Efimov V N *Yad. Fiz.* **12** 1080 (1970); *Phys. Rev. C* **44** 2303 (1991)
16. Jensen A S et al. *Rev. Mod. Phys.* **76** 215 (2004)
17. Nielsen E et al. *Phys. Rep.* **347** 373 (2001); Nielsen E, Fedorov D V, Jensen A S *Few-Body Syst.* **27** 15 (1999)
18. Hausmann R *Z. Phys. B* **91** 291 (1993)
19. Pieri P, Strinati G C *Phys. Rev. B* **61** 15370 (2000)
20. Petrov D S, Salomon C, Shlyapnikov G V *Phys. Rev. Lett.* **93** 090404 (2004)
21. Petrov D S, Baranov M A, Shlyapnikov G V *Phys. Rev. A* **67** 031601(R) (2003)
22. Bruch L W, Tjon J A *Phys. Rev. A* **19** 425 (1979)
23. Combescot R, Leyronas X, Kagan M Yu *Phys. Rev. A* **73** 023618 (2006)
24. Gor'kov L P, Melik-Barkhudarov T K *Zh. Eksp. Teor. Fiz.* **40** 1452 (1961) [*Sov. Phys. JETP* **13** 1018 (1961)]
25. Heiselberg H *Phys. Rev. A* **63** 043606 (2001)
26. Pieri P, Pisani L, Strinati G C *Phys. Rev. B* **72** 012506 (2005)
27. Astrakharchik G E et al. *Phys. Rev. Lett.* **93** 200404 (2004)
28. Burovski E et al. *Phys. Rev. Lett.* **96** 160402 (2006)
29. Kashurnikov V A, Prokof'ev N V, Svistunov B V *Phys. Rev. Lett.* **87** 120402 (2001)
30. Landau L D, Lifshitz E M *Statisticheskaya Fizika* (Statistical Physics) Pt. 1 (Moscow: Nauka, 1976) [Translated into English (Oxford: Pergamon Press, 1980)]
31. Kagan M Yu et al. *Phys. Rev. B* **57** 5995 (1998)
32. Bartenstein M et al. *Phys. Rev. Lett.* **92** 203201 (2004)
33. Combescot R, Kagan M Yu, Stringari S *Phys. Rev. A* **74** 042717 (2006); cond-mat/0607493
34. Hammer H-W, Son D T *Phys. Rev. Lett.* **93** 250408 (2004); Platter L, Hammer H-W, Meißner U-G *Few-Body Syst.* **35** 169 (2004)
35. Roati G et al. *Phys. Rev. Lett.* **89** 150403 (2002)
36. Modugno G et al. *Science* **297** 2240 (2002)
37. Anderson P W *Science* **235** 1196 (1987)
38. Laughlin R B *Phys. Rev. Lett.* **60** 2677 (1988); Fetter A L, Hanna C B, Laughlin R B *Phys. Rev. B* **39** 9679 (1989)
39. Fulde P *Electron Correlations in Molecules and Solids* 2nd ed. (Berlin: Springer-Verlag, 1993)
40. Shraiman B I, Siggia E D *Phys. Rev. B* **42** 2485 (1990)
41. Belinicher V I, Chernyshev A L, Shubin V A *Phys. Rev. B* **56** 3381 (1997)
42. Belinicher V I et al. *Phys. Rev. B* **51** 6076 (1995)
43. Kagan M Yu, Rice T M *J. Phys.*: *Condens. Matter* **6** 3771 (1994)
44. Plakida N M et al. *Zh. Eksp. Teor. Fiz.* **124** 367 (2003) [*JETP* **97** 331 (2003)]

PACS numbers: **42.62.–b**, **52.38.–r**, 52.50.Jm
DOI: 10.1070/PU2006v049n10ABEH006098

Lasers and high energy density physics at the All-Russian Research Institute of Technical Physics (VNIITF)

A V Andriyash, P A Loboda, V A Lykov, V Yu Politov, M N Chizhkov

1. Introduction

The build-up of high energy density physics (HEDP) as an independent area of research was caused by the development of nuclear weaponry. By the end of the 1980s and the beginning of the 1990s, the activity of research in this area sharply increased. The reason was the growth in importance, in the atmosphere of the nuclear test ban, of laboratory studies aimed at confirming the reliability and security of nuclear stockpiles. To this end, the high-power laser facility projects of National Ignition Facility (NIF) and Megajoule laser facility (LMJ — Laser Mégajoule) with a total energy of laser radiation approaching 1.8 MJ are being pursued by Lawrence Livermore National Laboratory (LLNL, USA) and Commissariat a l'Energie Atomique (CEA, France), respectively [1, 2]. In addition to research concerned with nuclear stockpile stewardship, there are plans to utilize these facilities to demonstrate the possibility of employing fusion ignition to solve energy problems: the goal is to implement fusion ignition of microtargets with an energy yield higher than 20 MJ and more than 10^{19} 14-MeV neutrons per flash. At the Russian Federal Nuclear Center (RFNC) 'All-Russian Research Institute of Experimental Physics' (VNIIEF in Russ. abbr.), it is planed to build a solid-state-laser ISKRA-6 facility with an energy of up to 300 kJ in a nanosecond pulse [3]. Another factor determining the increase in the pace of research in HEDP is the astonishing

progress in building compact lasers for generating high-power ultrashort pulses. In a number of countries (France, Germany, Great Britain, Japan, Russia, and the United States), lasers with a peak power of 10–100 TW in a 0.1–1-ps pulse have been developed. At the end of the 1990s, a petawatt laser (500-J energy with a pulse length of 0.5 ps) was built at LLNL [4]. Recently, petawatt lasers have also been launched in Great Britain (Vulcan) [5] and Japan [6]. These facilities are employed in studies on the ultrahigh-intensity ($10^{18}-10^{20}$ W cm^{-2}) laser–matter interaction and the production of relativistic electrons, gamma-ray photons, and high-energy ions (with energies up to several dozen megaelectron-volts per nucleon). The employment of high-power lasers with ultrashort pulse lengths also opens new possibilities for HEDP (the study of properties of matter at ultrahigh pressures and temperatures) and for research in inertial fusion (the concept of 'fast ignition' of thermonuclear targets).

This report provides a brief review of the work in HEDP done at the RFNC 'E I Zababakhin All-Russia Research Institute of Technical Physics' (VNIITF in Russ. abbr.) and related to experiments involving high-power laser facilities. Such work consists of, first, theoretical and computational approaches to computer simulation of certain laser assemblies for laser fusion (LF) experiments. An analysis of the results of such studies shows that such assemblies serve as an extremely sensitive tools for calibrating theoretical models and verifying the various HEDP computer codes (the interaction of laser radiation with matter, the development of hydrodynamic instabilities, modeling high-intensity hydrodynamic flows, etc.). In view of the important role that radiation transfer plays in HEDP, both in describing the relevant processes and in diagnosing high-temperature dense plasmas, we will cover some results of research in modeling the spectral characteristics of multiply charged ions and the opacity of high-temperature dense plasma. We will also present the results of experimental studies and theoretical and computational modeling of a wide circle of physical phenomena that take place during the interaction of high-power picosecond laser light with matter.

2. Laser fusion as an area of research in HEDP

Theoretical, computational, and experimental research in the field of fusion target ignition by laser radiation at VNIITF began in the 1970s on the initiative of L P Feoktistov, who worked in close collaboration with the P N Lebedev Physics Institute of the USSR Academy of Sciences (FIAN).

Over the years, interest in this work has not waned at VNIITF. What makes this research so interesting is the multitude of physical processes and states realized in the systems considered and their certain similarity to the phenomena usually associated with thermonuclear weapon. Experimental research in laser fusion produces unique information for HEDP, which is used to verify models and computer codes. For example, let us consider the laser assembly utilized in indirect-driven target compression, i.e., with conversion of laser radiation into X-rays. Complete calculation of such an assembly is extremely difficult. Generally, one needs to solve three-dimensional gasdynamic equations with spectral transfer of radiation in conditions of nonequilibrium laser plasma and with proper allowance for instability development and turbulent mixing in plasma. Figure 1 shows the typical geometry of the system at the instant of time corresponding to the peak X-ray radiation temperature at the fusion target surface in a two-dimensional calculation done by the SINARA computer program [7]. The complex nature of gasdynamic flows is clearly visible in this computer simulation. At the same time, experimental data on the dynamics of motion in such a system make it possible to calibrate the computer codes intended for modeling the gasdynamic flows with substantial strains and the propagation of X-ray radiation in systems with a complex geometry. Another area of recent research in the field of theoretical and computational modeling at VNIITF is the study of the attainability of fusion ignition in systems with indirect-driven target irradiation with laser energies comparable to those of the ISKRA-6 facility [8]. The possibility of fusion ignition of a cryogenic target with a beryllium ablator (similar to the target used for NIF [9]) was examined. Computational optimization done by the Era computer program [10] led to the following consistent values of the target parameters and the shape of the optimal time dependence of the blackbody radiation temperature needed for fusion: the outer target diameter, 1.115 mm; the thickness of the $Be_{0.98}Cu_{0.02}$ shell, 82.5 μm, and the thickness of the layer of deuterium–tritium (DT) ice on the inner surface, 40 μm (see Fig. 2a). For the found optimal time dependence of the radiation temperature with a maximum value of 360 eV, the calculated fusion energy yield from the target amounted to about 1.7 MJ, with the blackbody radiation energy absorbed by the target being about 30 kJ. The density of the targets under compression was as high as 300–600 g cm^{-3}, while the ion temperature of the fuel during fusion combustion exceeded 30 keV. The X-ray yield of photons with energies exceeding 10 keV

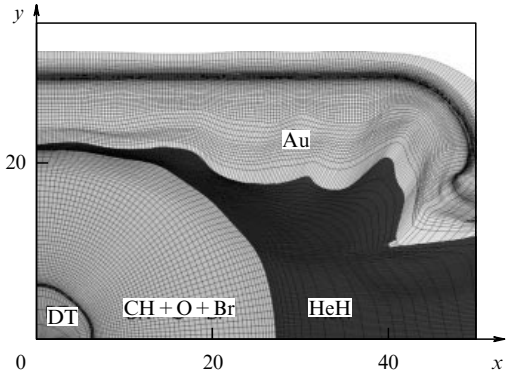

Figure 1. The geometry of the laser assembly and the spatial coordinates at the instant of time when the temperature of the radiation at the target surface reaches its maximum.

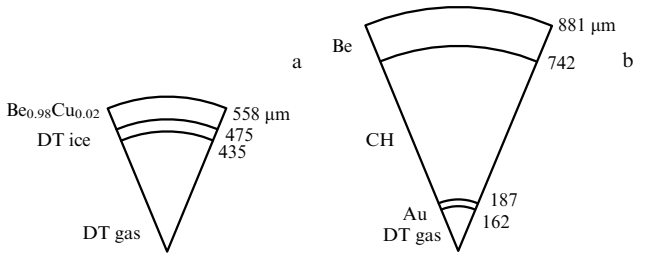

Figure 2. Targets for the ISKRA-6 facility: (a) the single-shell cryogenic target [8], and (b) the double-shell noncryogenic target [12].

amounted to about 150 kJ in the one-dimensional calculation, while the neutron yield was 6×10^{17}.

The sensitivity of the fusion energy yield to various factors is a special topic of research in computer simulations. To establish the criteria of purity of the target surface and uniformity of the flux of blackbody radiation falling on the target surface, two-dimensional calculations using the TIGR – Omega-3T computer program [11] were done, as well as one-dimensional calculations with allowance for turbulent mixing according to the $k\varepsilon$-model. According to calculated results reported by Chizhkov et al. [12], to reach a fusion energy yield from the target close to the results of one-dimensional calculations, the roughness of the inner surface of the beryllium shell must be no greater than 200 – 300 Å, which is three to five times smaller than in the case of the target at Los Alamos National Laboratory (LANL), used for ignition in the setup at NIF (the diameter of the target at NIF is 2.21 mm). The design of the laser assembly must guarantee the necessary symmetry of the radiation at the target surface (the total flux perturbation amplitude must not exceed 1%) and a time dependence of the radiation temperature of a special form with its maximum at about 360 eV, with the energy absorbed by the target being about 30 kJ. Thus, with a laser whose output energy is about 300 kJ, the energy conversion efficiency of the laser radiation (the ratio between the blackbody radiation energy transferred to the target and the laser energy) must be about 10%. Ensuring high energy conversion efficiency of laser radiation and high symmetry of the radiation at the target surface simultaneously is a difficult task. Calculations were also done for a noncryogenic target with two shells for the ISKRA-6 facility, a target similar to that used at NIF [13]. The target (see Fig. 2b) consists of an outer shell 140-μm thick made of pure beryllium with a diameter of 1.76 mm, and an inner 25-μm thick gold shell with a diameter of 0.37 mm. The shells are separated by a layer of low-density foam. The cavity at the target's center is filled with high-density deuterium – tritium gas at room temperature. The calculated fusion energy yield from the double-shell target amounted to 240 – 280 kJ, with the energy absorbed by the target being 60 – 70 kJ [12]. About 20% of the 300 kJ of the laser energy from the ISKRA-6 facility must be transferred to the target, which can be achieved by using the converter whose walls are made of a mixture of high-Z elements (what is known as cocktails). The radiation temperature required for the double-shell target considered amounts to 200 eV, which is much lower than the peak temperature (360 eV) for the cryogenic single-shell target. Two-dimensional calculations with the TIGR – Omega-3T program have demonstrated that the fusion energy yield from the noncryogenic target with two shells is close to that produced by one-dimensional calculations, with the amplitude of the perturbation in the form of the 12th harmonic on the outer surface of the gold and beryllium shells being up to 500 Å. The asymmetry of the blackbody radiation flux at the target surface must be smaller than 4% for a perturbation in the form of the fourth harmonic. The displacement of the shell centers must not exceed 1 – 2 μm. Calculations done at VNIITF point to the possibility of approaching very closely the ignition threshold of fusion targets with indirect-driven irradiation using facilities on the scale of ISKRA-6, which makes it possible to apply such a facility in studies of various HEDP processes (the development of instabilities, turbulent mixing, spectral radiation transfer, nonequilibrium processes, and so forth).

3. Modeling the spectral characteristics of multiply charged ions and the opacities of high-temperature dense plasmas

The development of theoretical and computational models of the interaction of X-ray radiation with matter received proper attention in the USSR at the atomic-weaponry centers in 1957, when in one of the first tests of a thermonuclear system built according to a new design a two-fold reduction in the time of operation of the thermonuclear device compared to the calculated time was recorded. This had uniquely indicated that the free path lengths of radiation in the structural materials of the charge were much smaller than those used in calculations. At the time, only Compton scattering, bremsstrahlung and photoionization absorption were taken into account in estimates of the radiation free path lengths. Ya B Zel'dovich noticed that bound – bound transitions might play a great role in the reduction of the lengths. A F Nikiforov and V B Uvarov, research workers at the Institute of Applied Mathematics (IAM) of the USSR Academy of Sciences, took an active part in improving the methods used in calculating the radiation free path lengths.

In their model [14], the contribution of bound electrons was evaluated from the solution of the Schrödinger equation with the Thomas – Fermi potential. Later on, new, more accurate, methods based on the modified Hartree – Fock – Slater model for the averaged ion were developed at IAM with the active participation of V G Novikov (see Ref. [11]; a list of references related to this problem can also be found in the monograph [15]).

For many years, the values of the free path lengths obtained on the basis of the Nikiforov's and Uvarov's model [14] were used in describing radiative transfer processes in HEDP problems.

In the early 1980s, the staff of VNIITF began developing their own physical models applied in calculating processes of the interaction between radiation and matter. At the time, such research stemmed from the pressing need to calculate the spectral absorption coefficients for various materials, including multicomponent mixtures, as applied to devices of unusual design being developed at the Institute.

At the first stage, when describing the state of matter the researchers used the semiclassical model of an averaged ion with an analytical intraatomic potential and adjustable parameters. This made it possible to obtain an explicit representation for the discrete electron energy levels [16]. Comparative calculations showed that the values of the total energies of isolated atoms, obtained in such a model, are in good agreement with data obtained by the Hartree – Fock – Slater method. Allowing for the diversity of the physical processes determining the position and shape of spectral lines, the researchers were guided by a simplified method for calculating the spectral absorption coefficients. When calculating discrete absorption in plasma with allowance made for the splitting and broadening of the spectral lines, they took into account only the statistical splitting related to fluctuations of the occupation numbers in the averaged ion model. Here, it was assumed that, within the spectral distributions obtained, the lines completely overlap due to the interaction with surrounding plasma [17]. Such a situation, as is known, is characteristic of high-density plasma, in which the confluence of the spectral lines corresponding to a specific one-electron transition $\mathrm{i} \to \mathrm{f}$ is examined in experiments, i.e., relatively broad envelopes of arrays of lines instead of separate peaks

Table 1. Absorption coefficient of the astrophysical mix [cm^2 g^{-1}].

T, keV	ρ, g cm^{-3}	Model [16]	Data [14]	Data [18]	Data [19]
0.1	0.2017	162	79.86	225.7	86.34
0.3162	0.0626	3.63	1.779	5.18	2.126
0.3162	0.06288	11.7	8.378	1.86	8.463
0.3162	6.31	25.4	21.25	18.56	20.15
1.0	1.977	0.585	0.533	0.6461	0.59

are observed. The simplicity of the model and the low computation time made it possible to easily generalize the model to the calculation of thermodynamic functions (and, correspondingly, of spectral lengths) of multicomponent systems consisting of a mixture of atoms of different chemical elements. A comparison of the results of the calculations (see Table 1) of the opacity of the astrophysical mix [16] with more accurate data [14, 18, 19] may serve as an illustration of the accuracy of the model.

In view of the efficiency of the simplified method and the rather good agreement with the results of more consistent and rigorous models, the given approach has been applied over the years to obtain estimates of the radiation free path lengths in various research.

In the mid-1990s, new studies in the field of the plasma spectroscopy of multiply charged ions (MCIs) began at the Institute. The goal was to develop X-ray diagnostics of laboratory plasma, to perform theoretical and numerical analysis of the characteristics of resonantly amplifying media, and to obtain more precise data on spectral opacities in matter. Today, the main areas of research in this field are as follows:

(1) Calculations of the spectral characteristics of multielectron ions with a high degree of ionization and the compiling of atomic databases.

(2) Development of physical and mathematical models for calculating the spectral characteristics of radiative transitions in MCIs, namely, the spectral line profiles for spontaneous emission, and the gain (absorption) coefficients, with allowance for the main mechanisms of line broadening in plasma and the effect of external fields on the kinetic processes of populations of ionic states.

(3) Development of physical and numerical models to calculate the spectral opacities of equilibrium multielectron MCI plasmas accounting for detailed and statistical description of the bound–bound and bound–free absorption spectra.

Concerning the first area of research, a large volume of computations of the spectroscopic characteristics of atoms and ions for various problems related to plasma diagnostics and the study of the schemes of X-ray lasers and for compiling atomic databases has been done at VNIITF. Calculations of the spectroscopic MCI characteristics are done by employing adapted and modernized versions of the best computer programs of the GRASP (General-purpose Relativistic Atomic-Stricture Program) family — that is, software aimed at calculating atomic structures by the multiconfiguration Dirac–Fock method [20, 21]. Extensive calculations of the spectroscopic characteristics have also been carried out to verify and extend the information accumulated in the online Spectr-W^3 database on spectral properties of atoms and ions, developed in 2001–2003 [22].

The web site of the Spectr-W^3 information reference system, operating on the Web freely accessible round-the-clock since May 2002, was integrated into the family of specialized databases for atomic and plasma physics on the Internet [23]. The information accumulated in the Spectr-W^3 database contains about 450,000 records and includes the experimental and theoretical data on ionization potentials, energy levels, wavelengths, radiation transition probabilities, and oscillator strengths, and, to a lesser extent, the parameters of analytical approximations of electron-collisional cross sections and rates for atoms and ions. To date, the Spectr-W^3 ADB is still the largest factual database in the world, containing the information on spectral properties of multiply charged ions.

In the second area of research, considerable progress has been achieved with the LineDM model [24] of calculating the profiles of spectral lines of arbitrary MCIs as applied to computations of local MCI emission and absorption spectra in high-temperature plasmas. This model, based on the atomic density matrix technique, takes into account the electron-impact, the ionic-quasistatic, the Doppler, and the radiative broadening of spectral lines in plasma, in addition to providing a detailed description of atomic structure. The initial data needed for calculating the population of Stark states are determined from computations taking advantage of the common radiation-collisional models.

In recent years, this model has found application in the solution of methodical and practical problems of laser-plasma diagnostics and in the development of high-luminosity sources of quasimonochromatic X-ray radiation. One example is the modeling of profiles of resonance lines of the [He]-like Ar XVII ion emitted from the Rydberg levels $1snl$ ($n = 5, \ldots, 10$), the modeling done with the aim of interpreting the results of laboratory experiments on irradiating gaseous argon cluster targets with subpicosecond laser pulses of durations ranging from 1.1 ps to 4.5 fs [25]. For instance, the experimental spectra recorded with a high resolution, $\lambda/\Delta\lambda \approx 3000-5000$, within the spectral range of $n^1P_1-1^1S_0$ ($n \geqslant 5$) radiative transitions in the Ar XVII ion demonstrated that as pulses became shorter the confluence of the close spectral lines for $n = 9 \rightarrow 1$ and $n = 10 \rightarrow 1$ ($\Delta\omega_{10p-9p} \approx 9.2$ eV) transitions becomes stronger. Thus, the main contribution to the time-integrated intensity of the line spectrum of the radiation emitted by plasma was provided by regions of ever increasing density with $N_e \geqslant (N_e^{IT})_{9,10}$ (densities according to the Inglis–Teller criterion for $n = 9, 10$). In Fig. 3 we compare the results of calculations of the profiles of spectral lines for $n = 9 \rightarrow 1$ and $n = 10 \rightarrow 1$ transitions in the Ar XVII ions, carried out for separate and combined allowance for the set of states with $n = 9$ and 10 for an equilibrium population distribution at $N_e \approx 2(N_e^{IT})_{9,10}$. Clearly, the profile of the spectral line for $n = (9 + 10) \rightarrow 1$ transition differs substantially from the sum of the profiles for $n = 9 \rightarrow 1$ and $n = 10 \rightarrow 1$. Overall, the profiles obtained are in qualitative agreement with the experimental spectra within the range of $n^1P_1-1^1S_0$ ($n \geqslant 5$) transitions in the Ar XVII ion and, therefore, were utilized for further quantitative analysis [25].

In the third area of research, a new numerical model Spectr, has been developed at VNIITF [26]. It is an implementation of a simplified variant of the Super Transition Array (STA) model [27, 28]. The STA model, based on what is known as the superconfiguration (SC) approach, makes it possible to describe the sum spectra of 'relativistic' one-electron transitions (with allowance for the total angular momentum j), formed by arrays of overlapping (unresolved) lines and photoionization continua, with a small number of

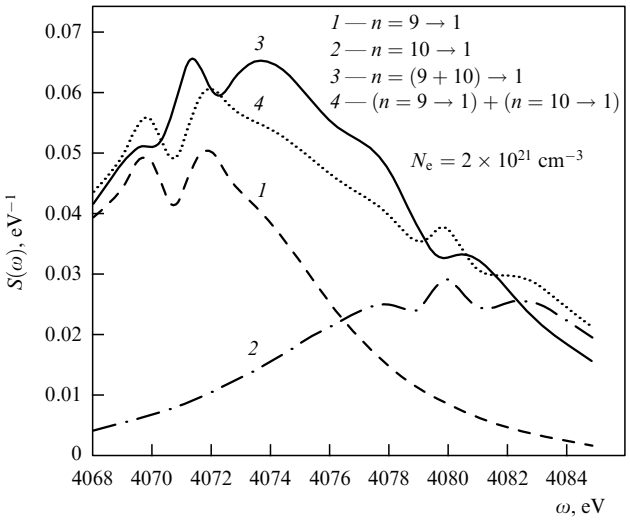

Figure 3. Profiles of the spectral lines for $n = 9 \to 1$, $n = 10 \to 1$, and $n = (9 + 10) \to 1$ transitions in Ar XVII ion in subpicosecond plasma of clustered argon at $T_e = 200$ eV and $N_e = 2 \times 10^{21}$ cm^{-3}, normalized to the total intensity of the sum profile for $n = (9 + 10) \to 1$.

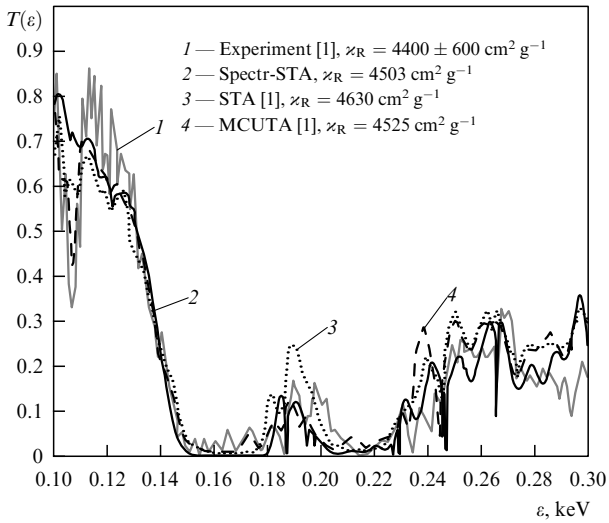

Figure 4. Spectral transmittances $T(\varepsilon)$ of the iron component of an Fe:NaF plasma layer 300-μm thick with an 80.2% iron weight content at $T = 59$ eV and the density $\rho = 0.0113$ g cm^{-3}.

STAs that combine all possible spectra of such transitions from groups of energy-adjacent configurations, or superconfigurations.

The simplified variant of the STA model implemented in the Spectr model represents a direct generalization of a more detailed description of the spectra of interconfiguration transitions in ions with allowance for the interaction between configurations. The characteristics of superconfigurations and arrays of spectral lines representing the one-electron transitions between them are built directly from the configuration characteristics on an optimal temperature grid. Here, the supershells comprising the superconfigurations of the ions combine all *nl*-shells with the same value of *n*, i.e., coincide with the atomic shells.

At present, all the configuration characteristics are calculated beforehand with the employment of single-particle and pair values for the one-electron states (orbitals), obtained by the Hartree – Fock method with allowance made for relativistic corrections (the HFR method) [29]. In the absorption spectrum of plasma, the STAs are represented by the Voigt profiles. The Gaussian component is responsible for statistical broadening — the widths and average-energy variances of configuration – configuration transition arrays and Doppler broadening. The homogeneous component takes into account the radiative and collisional broadening. The ionization balance is calculated by the Saha – Boltzmann equations with allowance for electron degeneracy and plasma nonideality effects which are described in the ion-sphere approximation in terms of the corrections to the ionization potentials and by truncating the partition functions.

The total spectral opacity $\varkappa(\varepsilon)$ is determined by the sum of absorption coefficients in the lines of STA transitions, of absorption coefficients in the photoionization and bremsstrahlung continua, and by Compton scattering.

As an example, we present in Fig. 4 the experimental data of Springer et al. [30] and the results of calculations of the spectral transmittance $T(\varepsilon) = \exp\left[-\varkappa(\varepsilon)\rho L\right]$ of the iron component of an Fe:NaF plasma layer 300-μm thick with the density $\rho = 0.0113$ g cm^{-3} and an 80.2% iron weight content at the temperature $T = 59$ eV in a photon energy range $\varepsilon = 100 - 300$ eV. Under these conditions, the opacity of iron plasma is determined by the discrete and photoionization absorption of ions with unfilled L and M shells. Clearly, the results obtained by the Spectr program are in very good agreement with the experimental data of Springer et al. [30] and the results of calculations done with the original STA model [27] and the more detailed model of interconfiguration transitions MCUTA (the model of unresolved transition arrays) with the configurations chosen by the Monte Carlo method [30] both in the spectrum $T(\varepsilon)$ and in the values of the group (on the interval $\varepsilon = 100 - 300$ eV) Rosseland opacities $\varkappa_R$.

4. Interaction of picosecond laser pulses and matter

In 2000, research involving the picosecond laser facility Sokol-P began at VNIITF [31]. The facility was built according to the standard scheme of amplification by chirp-modulated pulses. The rated power of the facility was 5 – 10 TW, with the energy of the laser radiation on the target being 5 – 8 J and the laser pulse duration amounting to 0.8 – 3 ps. The contrast of the main laser pulse with respect to the prepulse exceeded 10^9.

As is known, the plasma produced in the interaction of ultrashort strong laser pulses with matter is a source of fast electrons and ions, as well as X-ray radiation of high luminance. In this case, a significant part of the laser pulse energy (up to roughly 30%) may be transformed in the surface layers of the target into the energy of fast electrons, a fact corroborated by measurements of the absolute yield of hard X-ray radiation [32]. High-energy electrons ($E_e \geqslant 30$ keV), which possess high penetration power, may lead to a fast, nearly isochoric, heating of target layers of considerable thickness (about several micrometers or even more). This fact was used in a series of experiments in which the emission spectra of high-temperature dense plasmas of solid targets, irradiated with picosecond laser pulses generated by the Sokol-P facility, were studied.

4.1 X-ray radiation from laser targets

At the first stage of studies on the spectra of X-ray radiation from laser targets [33], the attention of the researchers was mainly focused on developing methods of measuring the spectral composition of the X-ray radiation and on determining the characteristic temperatures of the picosecond laser plasma and the depth to which the heat wave penetrates the target. Two types of targets were irradiated by laser light: massive homogeneous plates, and thin multilayer targets with a 'buried' radiation-emitting layer (the multilayer construction was chosen with the aim of suppressing the expansion of the plasma generating the X-ray radiation by the substance of the outer plates). Aluminium was used as the diagnosable material of the massive plate and the 'buried' layer in view of its relatively simple and well-studied atomic structure.

Two different spectrometers were utilized to record the X-ray spectra. First, the broadband spectrum of the continuum radiation emitted by the laser plasma over the range from 1 to ~ 17 keV was measured. This involved the employment of a seven-channel semiconductor spectrometer that implemented the technique of 'neutral' filters. Each detector of the spectrometer was covered with beryllium or aluminium foil of varying thickness, which ensured the selection of individual spectral intervals. The thicknesses of the first four filters of the spectrometer, which were optimized to the range of soft photon energies below 10 keV, amounted to $2-35$ mg cm^{-2}. The filters used in the harder spectral range were 100 to roughly 700-mg cm^{-2} thick.

In addition, a focusing von Hamos spectrograph with a crystalline dispersive element positioned at an observation angle of approximately 25° to the target plane was applied to measure the line spectra of hydrogenlike and heliumlike aluminium ions over the photon energy (ε) range from 1.4 to 2.5 keV.

To interpret the measured X-ray spectra under conditions where a massive target and microdots are to be irradiated with a picosecond pulse of the first harmonic of an Nd-laser, a series of theoretical and computational modelings was performed. The simulation proceeded from successive calculations of the radiation gas dynamics, level-by-level ion kinetics, and radiative transfer [34, 35]. The initial data for the computations were the geometrical parameters of the targets and the parameters of the irradiation pulse with a diameter of the focal spot $D_0 \sim 30-40$ μm, which corresponds to a peak flux density $q_0 \sim (5-8) \times 10^{17}$ W cm^{-2}. For a microdot, the thickness of the polyethylene plates was about 2.2 μm, and the thickness of the aluminium layer amounted to 4 μm.

Examples of the modelled X-ray spectra as compared to the experimental spectra for a massive target and a microdot with photon energies ranging from 0 to 8 keV are depicted in Fig. 5 [33]. These patterns show that in the case of a massive target the main contribution to the radiation intensity is provided by photorecombination on the Al^{+13} and Al^{+12} ions, while for a microdot the radiation yield is determined mainly by the hydrogenlike carbon ions; as a result, the intensity of the X-ray radiation from a microdot proves to be lower by an order of magnitude. The effective temperature of the X-ray spectrum in both cases is approximately the same and is estimated to be roughly 0.8 keV, which is in reasonable agreement with the measurement results.

The line spectra of the X-ray radiation emitted by hydrogenlike and heliumlike aluminium ions were also calculated within the framework of the modeling method briefly discussed above. For a massive target, these spectra are demonstrated, together with the experimental spectra for the sake of comparison, in Fig. 6. Qualitatively and, to a certain extent, quantitatively, the calculated absolute and relative intensities of the strongest resonance lines Ly_α, Ly_β, He_α, and He_β proved to be close to the measured magnitudes (differing by less than a factor of two).

4.2 Production of fast ions

The concept of fast ignition in thermonuclear microtargets is based on the employment of high-energy electrons generated in the interaction of short intense laser pulses with plasma. According to this approach, the heating of precompressed fuel to temperatures needed for initiating fusion ignition is presumed to be done with the energy released by fast electrons produced by an ultrashort laser pulse. However, experiments have shown that the interaction of such laser pulses with plasma is accompanied by ion acceleration. When the electron production efficiency is high, the fast ions may additionally heat the thermonuclear fuel. Hence, the study

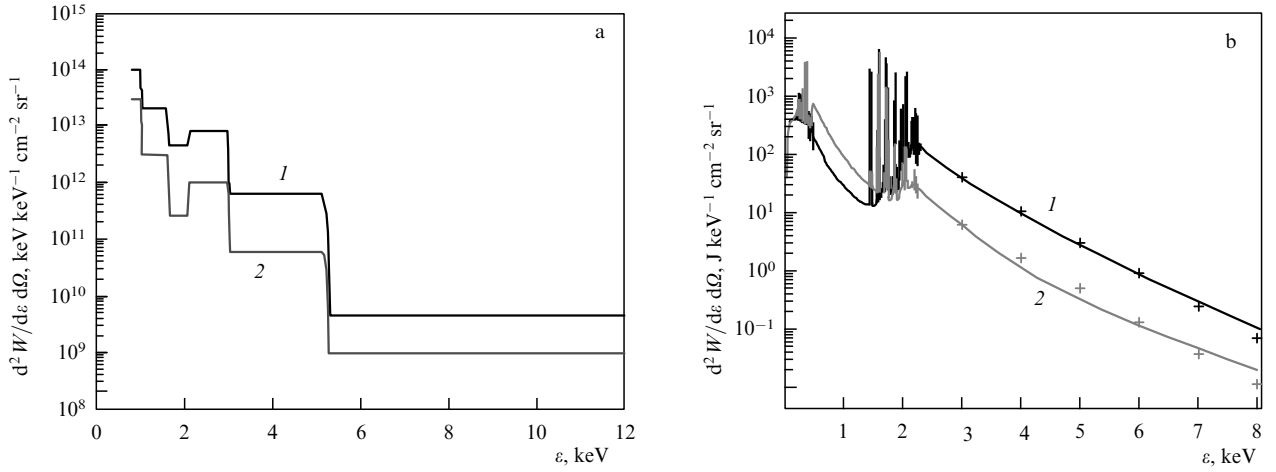

Figure 5. (a) Spectral distribution of the energy of soft X-ray radiation for a massive aluminium target (*1*), and a target with a 'buried' emitting aluminium layer 4.3-μm thick inside the polyethylene plates 2.2-μm thick each (*2*). (b) Calculated time-integrated emission spectra of the targets as in Fig. 5a at an angle $\theta_0 = 25°$ to the target plane with a laser pulse absorption efficiency $\eta = 0.05$. The symbols denote the exponential functions corresponding to $T_e = 0.8$ keV.

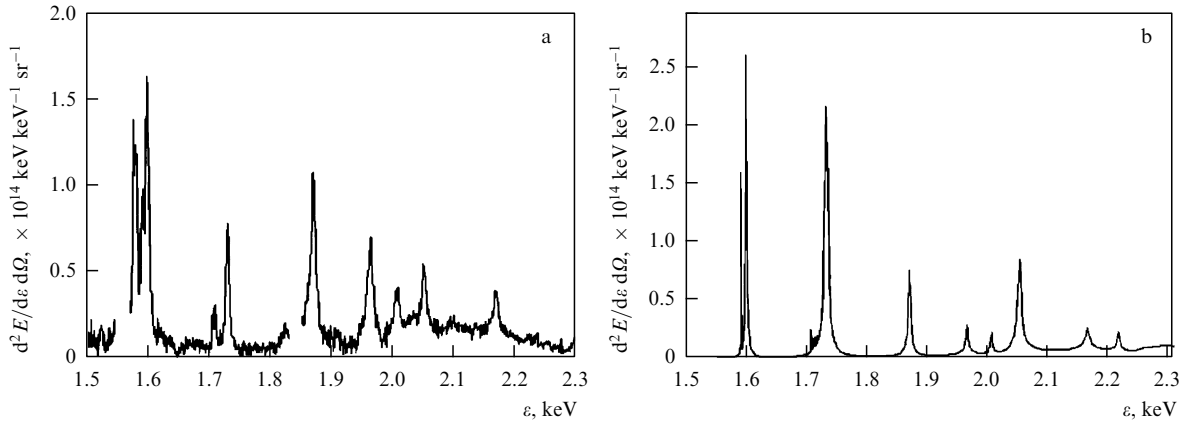

Figure 6. Experimental (a) and calculated (b) radiation spectra comprising the lines of H- and He-like ions of aluminium for a massive target.

of the mechanisms by which laser energy is transferred to target ions constitutes one of the areas of research in fast ignition.

To implement the various suggestions on the use of ions accelerated by a laser light in practical terms, we must study more thoroughly the mechanisms by which such ions are produced and specify the optimal conditions of target irradiation for an effective transfer of laser energy to ions. This has been the goal of a series of experimental studies involving the picosecond laser facility Sokol-P at VNIITF.

The irradiated targets were solid deuterated polyethylene $(CD_2)_n$ targets 5–300-μm thick and those of titanium deuteride–tritide $TiD_{0.5}T_{0.5}$ 5-μm thick on a copper substrate. The laser energy at the target surface amounted to 5–8 J, and the pulse duration was 0.8–2 ps. The peak intensity of radiation at the target ranged $(0.5-2)\times 10^{18}$ W cm^{-2}. Finally, the contrast of the picosecond prepulse in a time 12 ns before the arrival of the main pulse varied from 5×10^5 to 10^9.

The characteristics of the ions emerging from a target were measured by time-of-flight technique using semiconductor detectors [36], while the characteristics of the ions accelerated deep into the target were reconstructed from the results of neutron measurements [37]. The neutrons were produced in $D(d,n)^3He$ reactions (DD-neutrons) and $T(d,n)^4He$ reactions (DT-neutrons) when a beam of fast deuterons interacted with the deuterium and tritium nuclei of the target. The neutron yield was measured with scintillation detectors by the drawn-out recording technique, and neutron energies were determined by a time-of-flight detector.

The maximum energy of the deuterons accelerated at the irradiated surface away from the target amounted to about 3 MeV, while the average temperature of the fast deuterons was about 400 keV. The total energy of the accelerated deuterons varied from 10 to 100 mJ (through an angle of 2π). The efficiency of laser energy transfer to fast ions ranged 0.2–1.4%. A typical energy spectrum of deuterons used in such experiments is illustrated in Fig. 7.

The maximum yield of DD-neutrons during irradiation of single $(CD_2)_n$ targets was about 8×10^5, with the average value being 3×10^5. DT-neutrons were produced for the first time during irradiation of targets containing deuterium and tritium by ultrashort intense laser pulses. The maximum neutron yield from $TiD_{0.5}T_{0.5}$ targets amounted to about 2×10^6. The time-of-flight technique

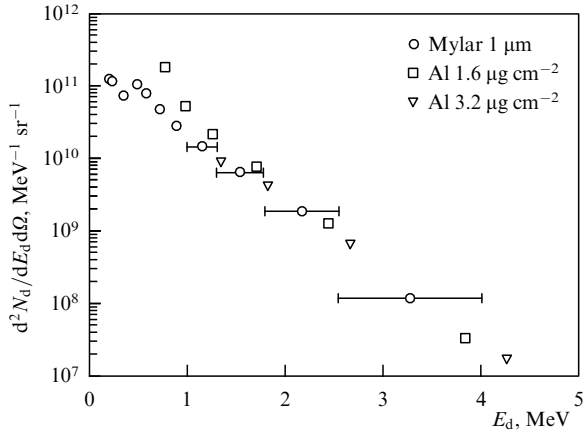

Figure 7. Characteristic energy spectrum of fast deuterons, measured at the front side of the irradiated target.

made it possible to identify neutrons from $D(d,n)^3He$ and $T(d,n)^4He$ reactions.

A simple model describing the interaction of a beam of fast ions with a target was utilized to study the ions accelerated deep into the target [37, 38]. The neutron yield was calculated by the formula

$$N_n = n_d \int_0^\infty dE_d^0 \frac{dN_d}{dE_d}(E_d^0) \int_0^{E_d^0} dE \frac{\sigma(E)}{|dE/dx|},$$

where n_d is the number of nuclei per unit target volume, dN_d/dE_d is the energy distribution of fast deuterons, σ is the reaction cross section, and dE/dx is the ion energy loss in the target. The energy spectrum of deuterons was assumed exponential with the temperature T_d:

$$\frac{dN_d}{dE_d} = \frac{N_d}{T_d}\exp\left(-\frac{E_d}{T_d}\right).$$

The efficiency of conversion of laser energy into the energy of fast ions was evaluated in the context of this model. At a deuteron temperature in the 100–500-keV range, 0.1–0.8% of the laser energy is transferred to the ions accelerated deep into the target from deuterated polyethylene, while 0.1–0.2% of the laser energy is transferred to the ions accelerated deep into the target from titanium deuteride–tritide.

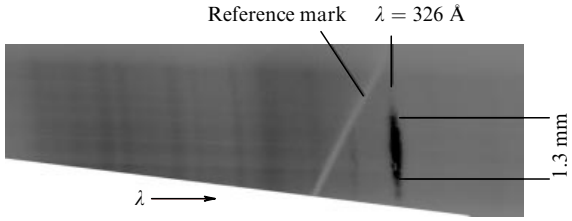

Figure 8. The spectrogram taken in the experiment with a 6-mm long target.

A number of experiments were carried out with additional targets. In experiments with a $TiD_{0.5}T_{0.5}$ target located at the rear of the irradiated $(CD_2)_n$ target, the neutron yield was found to be approximately an order of magnitude greater than in experiments with single $(CD_2)_n$ targets. An additional $TiD_{0.5}T_{0.5}$ target positioned in front of the irradiated $(CD_2)_n$ target yielded a 50-fold increase in the number of neutrons. A $(CD_2)_n$ target placed in front of another $(CD_2)_n$ target increased the neutron yield by a factor of three to five. The maximum recorded yield of DT-neutrons amounted to more than 10^7. Neutron measurements in experiments with additional targets made it possible to conduct an experimental estimation of the efficiency of laser energy transfer to the ions emerging from the target front side that agrees fairly well with the results of ion diagnostics.

The efficiency of conversion of laser energy into the energy of fast ions that was measured in experiments is not high enough for implementing the different suggestions concerning the use of the technique of laser acceleration of ions (fast ignition of thermonuclear targets, isotope recovery, and so forth). For such applications, the intensity of ultrashort laser pulses must exceed 10^{19} W cm^{-2}.

4.3 Lasing in the X-ray range

The Sokol-P laser facility has been used to study the laser X-ray effect involving 3p–3s transitions in Ne-like titanium ions [39]. Laser radiation with a wavelength of 1.054 μm was focused into a line 2 to 8-mm long and roughly 30-μm wide. Flat polished titanium plates were successively irradiated with two laser pulses: a prepulse 400-ps long, and a main pump pulse 4-ps long delayed (with respect to the first pulse) by 1.5 ns. The total laser energy was 8 – 10 J. The energy ratio in the nanosecond and picosecond laser pulses remained constant and equal to 1:3. When the target was short (from 2 to 4 mm), the experiments revealed an exponential build-up of the intensity of the line with the wavelength $\lambda = 326$ Å. Figure 8 portrays the spectrogram recorded in an experiment with a target 6-mm long. The small-signal gain of the laser X-ray radiation is estimated at about 30 cm^{-1}. Finally, the divergence of the laser X-ray beam was about 9 mrad.

5. Conclusions

In this report we have presented a short review of the experimental, theoretical, and computational studies done at VNIITF in the field of high energy density physics. Progress in this area of research can be attributed primarily to construction of the high-power picosecond laser facility Sokol-P and the development of complex physical and mathematical models, as well as computer programs making it possible to simulate the radiation gas dynamics of laser plasma.

One- and two-dimensional numerical calculations made it possible to analyze the conditions needed for the ignition of LF targets of various designs under conditions of indirect irradiation, including the parameters of the powerful ISKRA-6 facility under construction. The effect of roughness of the shell layers of targets and the inhomogeneity of blackbody radiation on their outer surface on the fusion energy yield has been studied. The rigid requirements to target quality, corresponding to the restrictions that the size of the roughness amplitudes must be no larger than 200 – 300 Å and the displacement of the shell center must be no more than 1 – 2 μm, have been substantiated.

As a result of a complex of investigations into the spectroscopy of MCI plasma conducted at VNIITF, original methods of calculating the spectroscopic characteristics of multielectron ions with the necessary accuracy have been developed, the freely accessible information-reference system based on the factual atomic database Spectr-W^3 was developed and is currently supported, and several physical and mathematical models that describe the spectral characteristics of radiative transitions and spectral opacities in equilibrium MCI plasmas have been implemented. These methods and models are being used at solving various applied problems of HEDP, while the Spectr-W^3 atomic database is being widely employed by specialists of scientific bodies from various countries.

The Sokol-P laser facility is used extensively for experimental research in converting the energy of optical photons into broadband, resonance, and laser X-ray radiation and into fluxes of fast neutrons. The possibility of producing multiply charged plasma with a density close to that of a solid has been explored in experiments with massive and multilayered aluminium targets and point focusing of a laser pulse whose intensity was in the $10^{17}-10^{18}$-W cm^{-2} range. The diagnostics of the parameters of such plasma was done on the basis of a theoretical and computational analysis of the time-integrated measurements of X-ray radiation spectra. By varying the fraction of the absorbed laser energy within reasonable limits, it was possible to match the calculated and experimental values of the spectra in the range of soft photon energies. Qualitative agreement in the spectral distributions of the intensity in the resonance lines of hydrogenlike and heliumlike aluminium ions has also been achieved. The characteristic temperature of picosecond laser plasma was estimated to be about 0.8 keV. The systematic discrepancy between the results of computations and measurements for the hard spectral range with photon energies of about 20 keV is an indication that bremsstrahlung of fast electrons dominates within this range but was not taken into account by the model.

New research in diagnosing the fluxes of fast particles in conditions of high-power picosecond irradiation of targets of deuterated polyethylene and titanium has begun. Technologies used in fabricating the targets and the methods applied to record thermonuclear neutrons have been perfected. Neutron yields of up to 10^6-10^7 per pulse of target irradiation have been registered, and this does not contradict the results of modeling this phenomenon in the conditions of the experiments conducted at the Sokol-P facility.

A series of experiments on generating laser X-ray radiation with a wavelength of 326 Å in plasma of Ne-like titanium ions has been conducted. The technology of focusing into a line the pulses used to irradiate a flat target has been implemented. The length of the line is up to 1 cm, and its

width is 30 – 50 μm. A dependence of the intensity of generation on the target length has been examined experimentally. Saturation of lasing has been achieved, and a reliable estimate of the small-signal effective gain (~ 30 cm^{-1}) has been obtained; the maximum energy of laser X-ray radiation does not exceed approximately 1 μJ.

References

1. Lindl J *Phys. Plasmas* **2** 3933 (1995)
2. Andre M L, in *IFSA 99 — Inertial Fusion Sciences and Applications* (The Data Science Library, Vol. 2, Eds C Labaune, W J Hogan, K A Tanaka) (Amsterdam: Elsevier, 2000) p. 32
3. Kirillov G A et al. *Laser Part. Beams* **18** 219 (2000)
4. Perry M D et al. *Opt. Lett.* **24** 160 (1999)
5. Norreys P A, Krushelnick K M, Zepf M *Plasma Phys. Control. Fusion* **46** B13 (2004)
6. Tanaka K A et al. *Plasma Phys. Control. Fusion* **46** B41 (2004)
7. Gadzhieva V V et al. *Voprosy At. Nauki Tekh. Ser. Mat. Mod. Fiz. Prots.* (3) 25 (2000)
8. Karlykhanov N G et al. *Pis'ma Zh. Eksp. Teor. Fiz.* **79** 30 (2004) [*JETP Lett.* **79** 25 (2004)]
9. Wilson D C, Krauser W J, in *Laser Interaction with Matter: Proc. of the 23rd European Conf.* (Inst. of Phys. Conf. Ser., No. 140, Ed. S J Rose) (Bristol: IOP Publ., 1995) p. 459
10. Zuev A I *Zh. Vychisl. Mat. Mat. Fiz.* **32** 82 (1992) [*Comput. Math. Math. Phys.* **32** 70 (1992)]; Barysheva N M et al. *Zh. Vychisl. Mat. Mat. Fiz.* **22** 401 (1982) [*Comput. Math. Math. Phys.* **22** 156 (1982)]
11. Shushlebin A N et al., in *Vychislitel'nye Tekhnologii* (Computational Techniques) Vol. 4, No. 13 (Novosibirsk: Institut Vychislitel'nykh Tekhnologii SO RAN, 1995) p. 336
12. Chizhkov M N et al. *Laser Part. Beams* **23** 261 (2005)
13. Amendt P et al. *Phys. Plasmas* **9** 2221 (2002)
14. Nikiforov A F, Uvarov V B *Dokl. Akad. Nauk SSSR* **191** 47 (1970) [*Sov. Phys. Dokl.* **15** 191 (1970)]
15. Nikiforov A F, Novikov V G, Uvarov V B *Kvantovo-statisticheskie Modeli Vysokotemperaturnoi Plazmy: Metody Rascheta Rosselandovykh Probegov i Uravnenii Sostoyaniya* (Quantum-Statistical Models of High-Temperature Plasma: Computing Methods for Rosseland Lengths and Equations of State) (Moscow: Fizmatlit, 2000) [Translated into English: *Quantum-Statistical Models of Hot Dense Matter: Method for Computation and Equation of State* (Basel: Birkhäuser Verlag, 2005)]
16. Andriyash A V, Simonenko V A *Fiz. Plazmy* **14** 1201 (1988) [*Sov. J. Plasma Phys.* **14** 703 (1988)]
17. Stein J, Shalitin D, Ron A *Phys. Rev. A* **31** 446 (1985)
18. Cox A N, Stewart J N, Eilers D D *Astrophys. J. Suppl. Ser.* **11** 1 (1965)
19. Carson T R, Mayers D F, Stibbs D W N *Mon. Not. R. Astron. Soc.* **140** 483 (1968)
20. Dyall K G et al. *Comput. Phys. Commun.* **55** 425 (1989)
21. Parpia F A, Fischer C F, Grant I P *Comput. Phys. Commun.* **94** 249 (1996)
22. Loboda P A et al., in *Proc. XXVIII European Conf. on Laser Interaction with Matter: ECLIM, Rome, Italy, 6 – 10 September 2004*, p. 383; SPECTR-W^3, http://spectr-w3.snz.ru
23. WIS List of Databases for Atomic and Plasma Physics, http://plasma-gate.weizmann.ac.il/DBfAPP.html
24. Loboda P A et al. *Laser Part. Beams* **18** 275 (2000)
25. Magunov A I et al. *Pis'ma Zh. Eksp. Teor. Fiz.* **74** 412 (2001) [*JETP Lett.* **74** 375 (2001)]
26. Loboda P A et al. *J. Phys. A: Math. Gen.* **39** 4781 (2006)
27. Bar-Shalom A et al. *Phys. Rev. A* **40** 3183 (1989)
28. Bar-Shalom A, Oreg J, Goldstein W H *Phys. Rev. E* **51** 4882 (1995)
29. Cowan R D *The Theory of Atomic Structure and Spectra* (Berkeley: Univ. of California Press, 1981)
30. Springer P T et al. *Phys. Rev. Lett.* **69** 3735 (1992)
31. Dmitrov D A et al., in *Proc. XXVIII European Conf. on Laser Interaction with Matter: ECLIM, Rome, Italy, 6 – 10 September 2004*, p. 591
32. Wharton K B et al. *Phys. Rev. Lett.* **81** 822 (1998)
33. Potapov A V et al., in *Tezisy 11-i Vseross. Konf. po Diagnostike Vysokotemperaturnoi Plazmy* (Digest of 11th All-Russia Conf. on High-Temperature Plasma Diagnostics), *Troitsk, Moscow region, June 13 – 18, 2005* (Moscow: RNTs 'Kurchatovskii Institut', 2005)
34. Politov V Yu, Lykov V A, Shinkarev M K *Proc. SPIE* **1928** 157 (1993)
35. Politov V Yu, Potapov A V, Antonova L V *Laser Part. Beams* **18** 291 (2000)
36. Andriyash A V et al. *Fiz. Plazmy* **32** 156 (2006) [*Plasma Phys. Rep.* **32** 135 (2006)]
37. Andriyash A V et al. "Izuchenie generatsii neitronov v T(d, n)^{4}He i D(d, n)^{3}He reaktsiyakh na 10 TW pikosekundnoi lazernoi ustanovke Sokol-P" ("Study of neutron production in T(d, n)^{4}He and D(d, n)^{3}He reactions using the 10-TeV picosecond Sokol-P laser facility"), in *VIII Zababakhinskie Nauchnye Chteniya* (8th Zababakhin Scientific Readings), *Snezhinsk, 2005*; http://www.vniitf.ru/rig/konfer/8zst/plenar/plen.htm
38. Bychenkov B Yu, Tikhonchuk V T, Tolokonnikov S V *Zh. Eksp. Teor. Fiz.* **115** 2080 (1999) [*JETP* **88** 1137 (1999)]
39. Andriyash A V et al. *Kvantovaya Elektron.* **36** 511 (2006) [*Quantum Electron.* **36** 511 (2006)]

PACS numbers: 05.10.Ln, 05.70.Jk, 75.40.Cx
DOI: 10.1070/PU2006v049n10ABEH006099

Monte Carlo studies of critical phenomena in spin lattice systems

A K Murtazaev

1. Introduction

The basic ideas of modern phase transition and critical phenomena theories are those associated with and involved in the scaling and universality hypotheses and renormalization group theory [1, 2].

Although it was believed until very recently that static phase transitions and critical phenomena have been fully explored and do not really need anything more in terms of theory, now the study of frustrated systems, magnetic superlattices, and spin systems with quenched nonmagnetic disorder shows that this is by far not the case [2 – 4].

Applied to such systems, traditional theoretical and experimental methods run into serious difficulties in an attempt to calculate critical parameters and to uncover the nature and peculiarities of critical behavior (including the mechanisms behind them), which led to the intense use of Monte Carlo (MC) methods in studies of phase transitions and critical phenomena in these systems [3 – 5].

The subject matter of this report is the critical behavior of the 3D Ising model with quenched nonmagnetic order for the example of cubic lattice and that of a model that was suggested to describe a real iron – vanadium superlattice $[Fe_2/V_{13}]_L$.

There are quite a number of reasons for interest in the critical behavior of such systems and their models. An actively discussed topic in the field has been that of how quenched nonmagnetic disorder affects the critical properties of spin lattice systems [2 – 4, 6 – 8]. In an important step, the so-called Harris criterion was developed within the framework of renormalized perturbation theory, which predicts, on a qualitative level, when and whether a particular impurity is of great concern in determining critical behavior [9]. According to this criterion, nonmagnetic disorder does play a role only in the situation when the specific heat critical exponent is positive, $\alpha > 0$: a condition which is satisfied only if the